Space Shuttle Entry Flight Control Off-Nominal Design Considerations

G. P. Bayle*
Rockwell International, Downey, California

The Shuttle Orbiter entry flight control system (FCS) was designed to meet certain specific performance requirements for given aerodynamics, line replaceable unit (LRU) tolerances, and flight envelopes. Further consideration was given in the design to provide for design assessment requirements under stress conditions. This paper addresses the off-nominal design considerations by providing a definition of the design performance requirements and the conditions under which these requirements are to be met. The approach taken in the classification of the aerodynamic uncertainties are given and the sensitivity of the flight control stability margins to aerodynamics is presented. Finally, the flight control verification process that was undertaken and a comparison of flight test results to predicted performance are discussed.

Introduction

A DISCUSSION of the off-nominal considerations imposed on the entry FCS in preparation for commit-to-flight on the first Orbiter flight test (OFT) is presented in this paper.

Shuttle Orbiter Flight Control Requirements

The flight control requirements, classified in three basic performance levels consisting of levels 1, 2, and design assessment, are defined as follows.[1] Level 1 performance consists of stability margins where the high-frequency crossover is 6 dB and a 30-deg phase with a low-frequency crossover of 12 dB. The pilot rating (Cooper Harper) should be 3 or less, while the step response should be within specified envelopes, as illustrated in Fig. 1. Level 2 performance consists of stability margins reduced to 4 dB and a 20-deg phase with large signal operation stable. The pilot rating (Cooper Harper) should be 6 or less. Design assessment should have performance such that no loss of vehicle prevails.

The conditions under which these requirements are to be maintained are: winds of steady-state values of 95% and 99% directional (worst month), selected flight application of discrete gusts, turbulence, and wind shear. Operational/OFT aerodynamic uncertainties will utilize lift-to-drag ratio plus pitching moment coefficient and stability derivatives where operational uncertainties represent the reduced magnitude of uncertainties to eventually be associated with operational flight. OFT uncertainties represent the larger uncertainties associated with the early phase preparation of flight testing. Allow worst-on-worst combinations of each previous element. Aero uncertainties, reaction control system (RCS)/aerodynamic interaction, bent airframe, and $Y_{c.g.}$ offsets will be treated as uncorrelated. Failures will be defined as: one fault—level 1 performance except air data loss (one side), level 2; and two faults—level 2 except for the loss of two RCS jets, which will be level 1; and two auxiliary power units' (APU) loss will be design assessment. The composite of the conditions that constitute a level 1, 2, or design assessment level of performance are classified according to wind magnitude of 0-99%, aerodynamic uncertainties and LRU tolerances, and apply for nominal and $\pm 3\sigma$ trajectory dispersions. This reflects the effect of atmospheric conditions, lift-to-drag ratio, and winds. They are independent of center-of-gravity locations and bent airframe conditions.

Definition of Off-Nominal Aerodynamics

Wind tunnel aerodynamic data[2] reduction has resulted in probable aerodynamic uncertainty bands about each of the basic aerodynamic coefficients. These bands have led to rectangular uncorrelated uncertainties and elliptical correlated uncertainties, as shown in Fig. 2. These uncertainties have been grouped into seven lateral variation (LVAR) sets: 2, 9, 10, 12, 19, 20, and 23. These sets were established to represent high and low Cn_β dynamic, high and low aerodynamic control gain, minimum and maximum aerodynamic surface controllability (coalignment of aerodynamic control effector vectors), and critical lateral trim (coalignment of sideslip and aileron vectors). The sensitivity of the aerodynamic uncertainties to controllability is further compounded by the aerodynamic sensitivity to angle of attack.

The flight control performance aerodynamic considerations consist of:

1) Coalignment of yaw jets and aileron is critical for lateral control and is further aggravated by an increase in dynamic pressure, which results in decreased jet effectiveness and an increase in jet uncertainty bounds, which results in further aileron yaw jet coalignment.

2) Coalignment of sideslip and aileron is critical for lateral trim, which is further aggravated by decreased angle of attack.

Sensitivity of Flight Control to Off-Nominal Conditions

The FCS was designed to operate within the conditions and requirements stated previously. The descent profiles consist of a basic entry and a glide-return-to-launch site (GRTLS), shown in Fig. 3. The vehicle velocity attitudes and dynamic pressure profiles for these two missions are shown in Figs. 4 (entry) and 5 (GRTLS). The control effectors consist of reaction jet control during preatmospheric flight and a combination of reaction jets and aerodynamic surfaces during postatmospheric flight, as illustrated in Fig. 6. The method utilized in establishing the flight control design and obtaining

Presented as Paper 82-1602 at the AIAA Guidance and Control, Atmospheric Flight Mechanics, and Astrodynamics Conference, San Diego, Calif., Aug. 9-11, 1982; submitted Aug. 9, 1982; revision received April 14, 1983.

*Supervisor, Design for Entry Systems and Flight Operations.

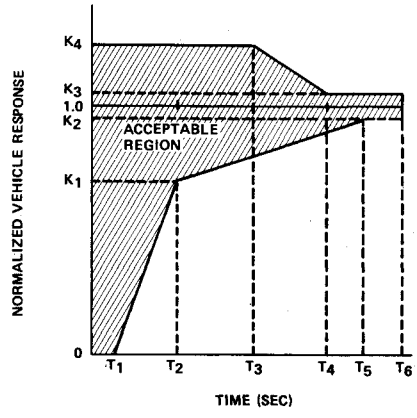

Fig. 1 Generalized step response.

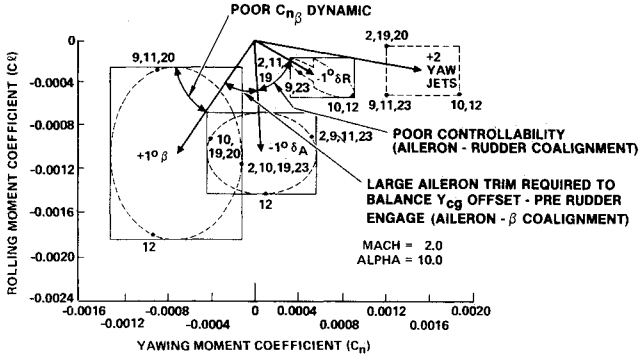

Fig. 2 Lateral aerodynamic uncertainties.

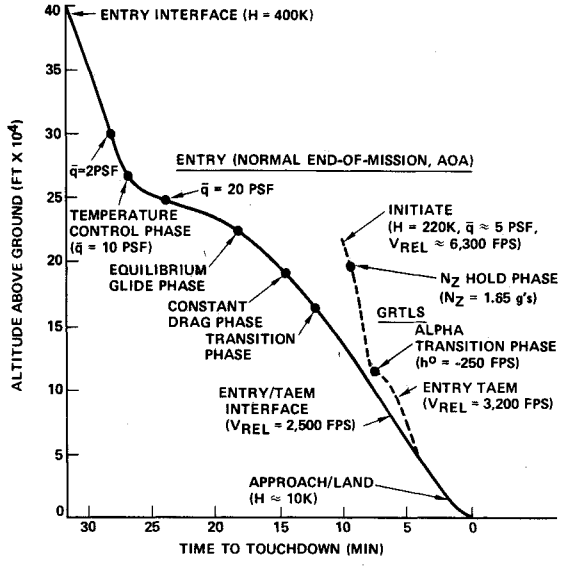

Fig. 3 Nominal entry/GRTLS flight profiles.

the flight control performance was to Monte Carlo the effect of winds, lift-to-drag ratio uncertainties and atmospheres, and create the flight envelopes shown in Figs. 7 and 8. Also shown in the figures are the verification test cases within the flight envelopes. The critical control region occurs when the aerodynamic vector approaches coalignment as previously discussed. This condition begins below Mach 6 and prevails until the rudder has acquired sufficient authority to re-establish positive control around Mach 1.0 where the yaw reaction jets are turned off.

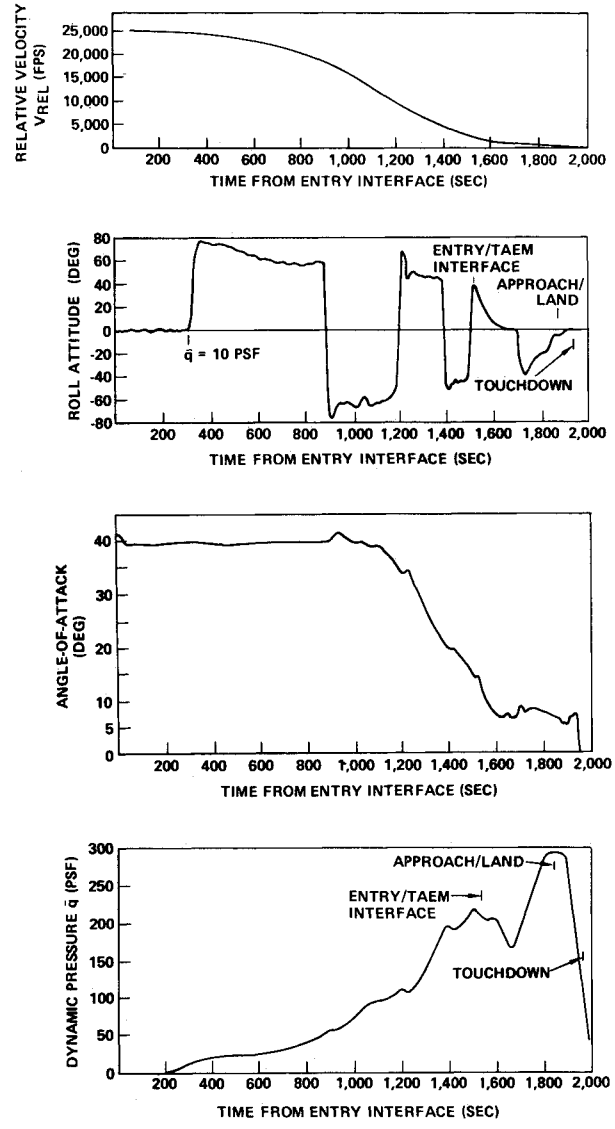

Fig. 4 Entry profile.

The sensitivity of aerodynamic uncertainties to flight control performance is best illustrated by referring to Fig. 9, where the progressive destabilizing effect of aerodynamic uncertainties LVAR 9 is evident by starting with the nominal aerodynamic (damping ratio of 0.82) and adding incrementally the constituents of LVAR 9. As shown, the damping ratio is drastically reduced by the aero partials of C_{ℓ_A} (rolling moment caused by aileron, increments 5 to 6) and $C_{\ell_{yj}}$ (rolling moment caused by yaw jets, increments 11 to 12). The composite effect of LVAR 9 is to force a well-behaved response with nominal aerodynamic coefficients into a slightly unstable response (damping ratio less than zero) as shown.

Another method used to better understand the effect of aerodynamic uncertainties is the mapping of the neutral damping contours in the lateral rolling, yawing coefficient plane, or the rolling, yawing yaw reaction jet moment plane as shown in Fig. 10. The same condition previously discussed is used consisting of LVAR 9 at Mach 5 with a dynamic pressure of 190 psf. This condition represents a point along the $+3\sigma$ flight envelope of Fig. 7. The mapping of the neutral damping contour of Fig. 10 is achieved by scanning the yaw reaction jet vector until the instability boundary is found with every loop of the FCS closed. This method clearly illustrates the effect of the yaw jets vector upon stability. The system is stable with nominal yaw jets and becomes slightly unstable at a frequency

of 1.43 rad/s with the LVAR 9 yaw uncertainties and a dynamic pressure of 190 psf. If the dynamic pressure is increased to 400 psf, the system becomes unstable as shown.

The formal stability verification analyses were performed using DIGIKON, a Z-domain stability analysis program. All of the test cases identified in Fig. 7 were performed. Since the critical stability region occurs in the Mach 5 to 2 region, representative stability margins for nominal and off-nominal aerodynamics are presented in the Nichols plots shown in Figs. 11 and 12. As shown, the most severe lateral variation is that of LVAR 9. These data were obtained at Mach 5.1 and 3.4 along a nominal profile. Marginal stability occurs with LVAR 9 for 3σ trajectory profiles, which was previously discussed, because of the resulting increase in dynamic pressure, as presented in Fig. 10. This condition represents a design assessment performance and was further assessed in the real-time simulator in the Flight Systems Laboratory (FSL), where the instability was found to be of a low amplitude and short duration, and is, therefore, acceptable for this worst-on-worst condition. In addition to the Nichols plots, step responses were performed as shown in Fig. 13 for nominal lateral aerodynamics along a nominal trajectory. These responses justified the stability analyses and verified that system nonlinearities on sensors and actuators did not degrade system performance beyond that predicted by describing functions.

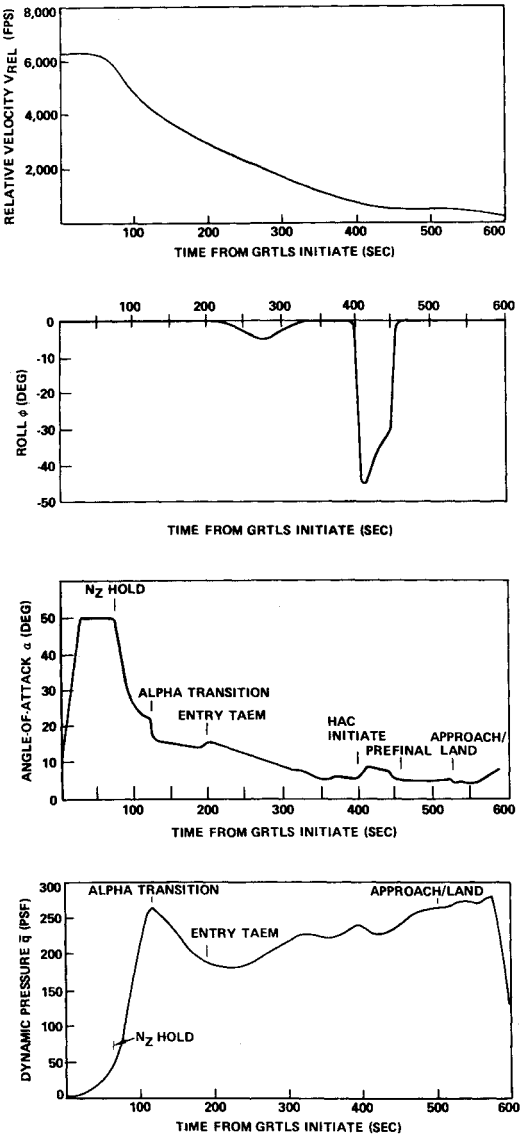

Fig. 5 GRTLS profile.

Similar emphasis was placed on the pitch axis, but since it is more benign than the lateral axes, it is not discussed in this paper.

In addition to the stability analyses discussed, real-time man in the loop (MIL) was performed in the FSL with the same aerodynamic uncertainties, and forcing the trajectory excursions by the inclusion of lift-to-drag uncertainties, winds, and atmospheres. The FSL results substantiate the results of these analyses and, therefore, are not included in this paper.

Flight Control Verification Process

The flight control verification consisted of the use of stability margin (DIGIKON), step response at a stationary point along a trajectory profile, and real-time MIL simulation

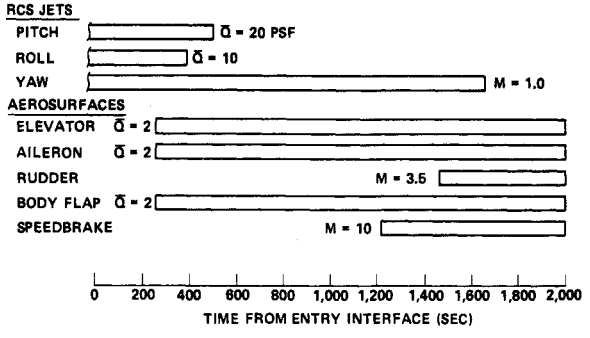

Fig. 6 Effector utilization.

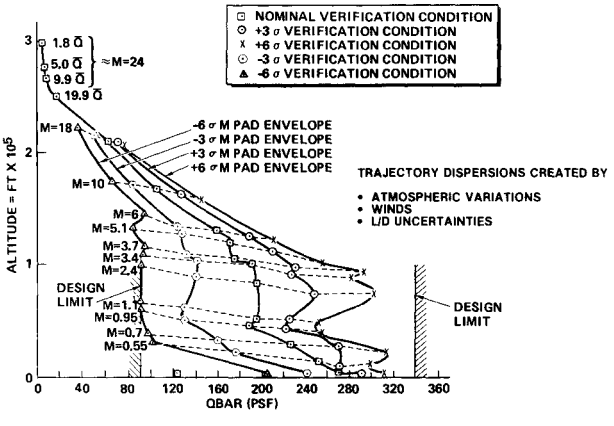

Fig. 7 Flight envelope, entry flight.

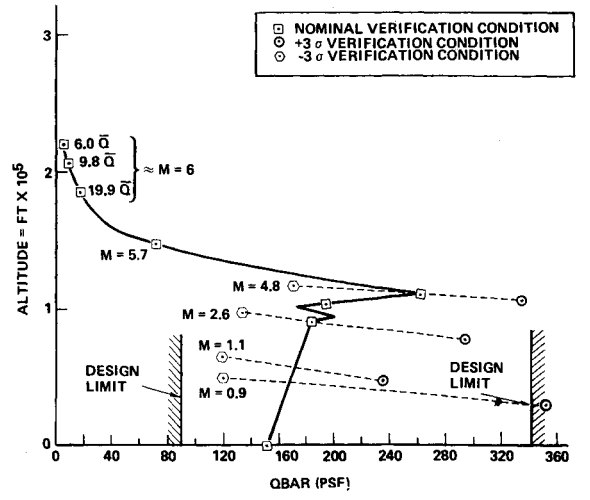

Fig. 8 Flight envelope, GRTLS flight.

performed in FSL, which included the Shuttle Orbiter multiplexer/demultiplexer (MDM), general-purpose computer (GPC), and flight software. The process used was to proceed with nominal aerodynamics, and, if successful, proceed with the testing of OFT aerodynamic uncertainties. Use of operational uncertainties was to be used only in the event of a failure condition with OFT uncertainties, as shown in Fig. 14. The alternate path was not found necessary. The only step necessary was to fall back to seasonal wind and atmosphere in support of the first flight, to reduce dynamic pressure, and maintain a stability margin with LVAR 9 aerodynamic uncertainties.

Flight Test Results

The first orbital flight test demonstrated nominal trajectory and nominal aerodynamics with the exception of the yaw jet aerodynamic interaction at the first roll maneuver, the static pitching moment, and the lift-to-drag ratio in ground effect, which were found to be less than predicted. Also noted was evidence of less aileron roll effectiveness and greater rudder

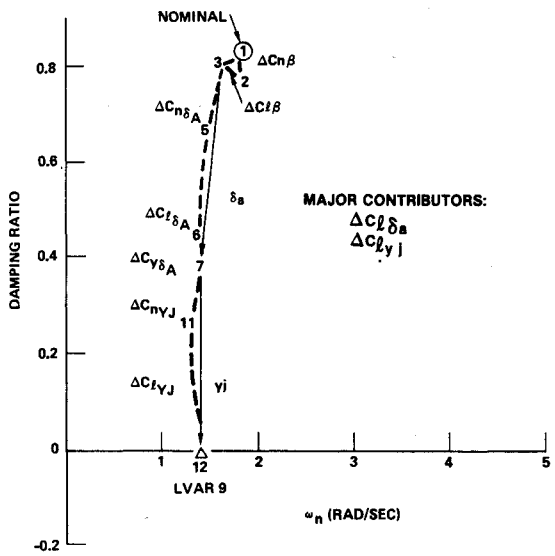

Fig. 9 Damping ratio vs natural frequency.

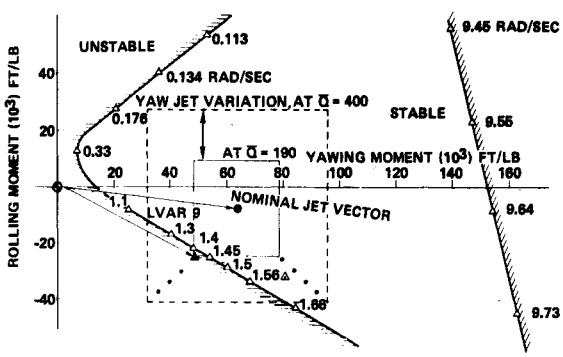

Fig. 10 Yaw jet torque dynamic stability boundary.

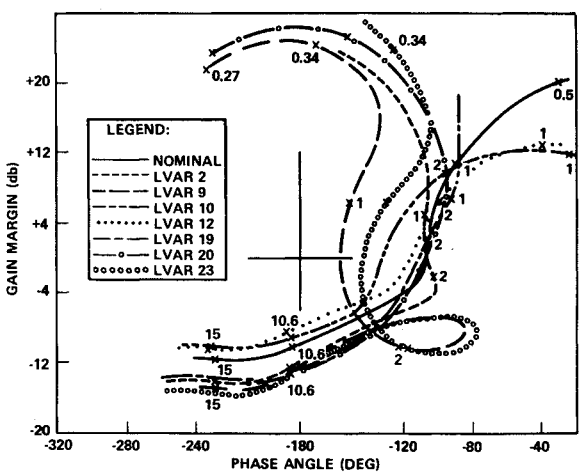

Fig. 11 Nichols plot; open-loop yaw jet, $M = 3.4$.

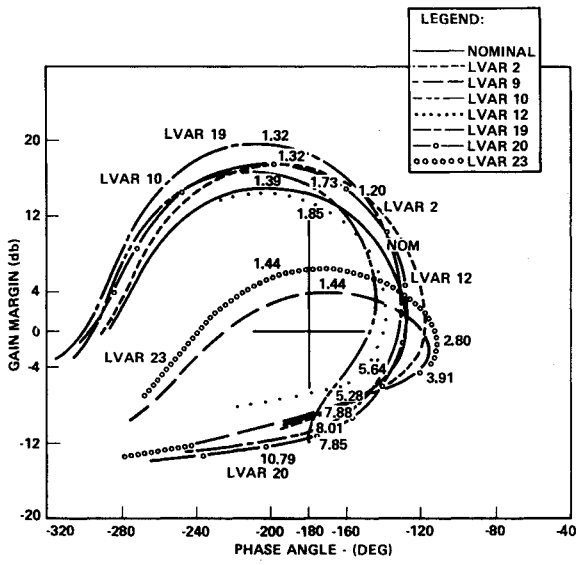

Fig. 12 Nichols plot; open-loop aileron, $M = 3.4$.

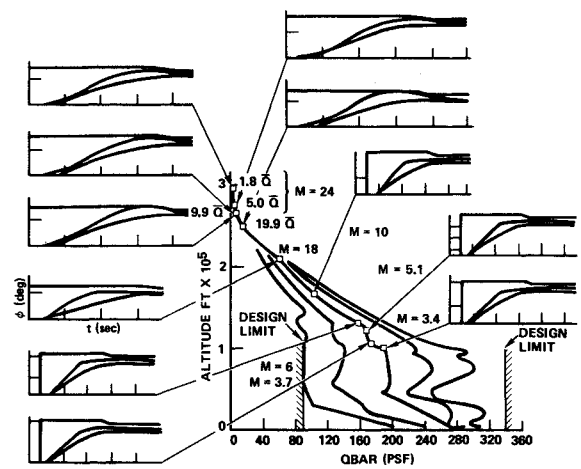

Fig. 13 Body roll angle response (entry/TAEM/AL).

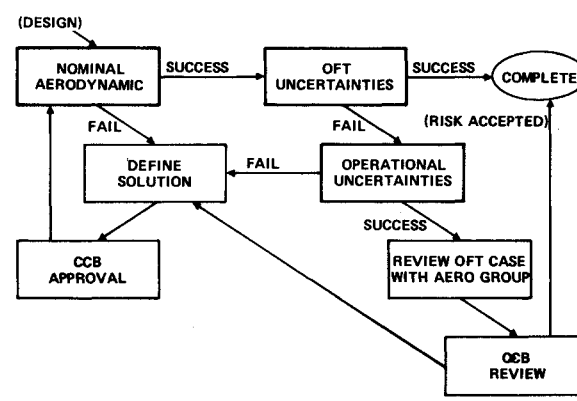

Fig. 14 Verification response.

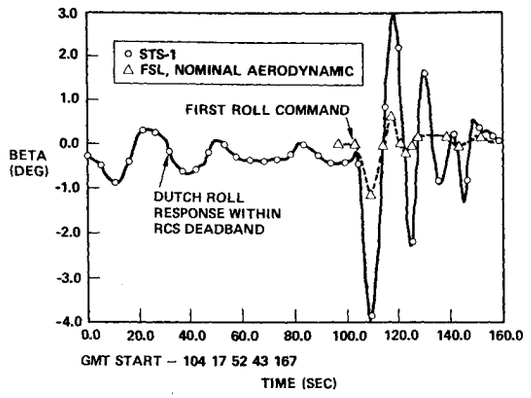

Fig. 15 Sideslip comparison of STS-1 and FSL data.

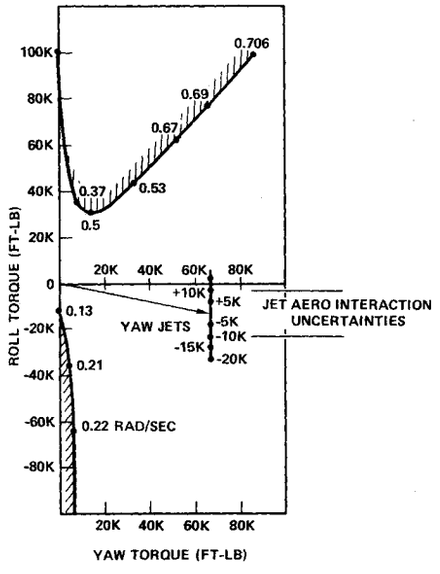

Fig. 16 First roll maneuver stability with β filter.

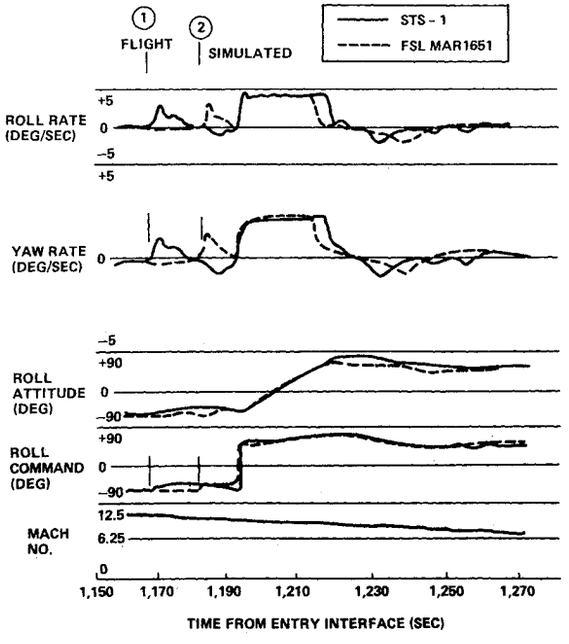

Fig. 17 Second reversal.

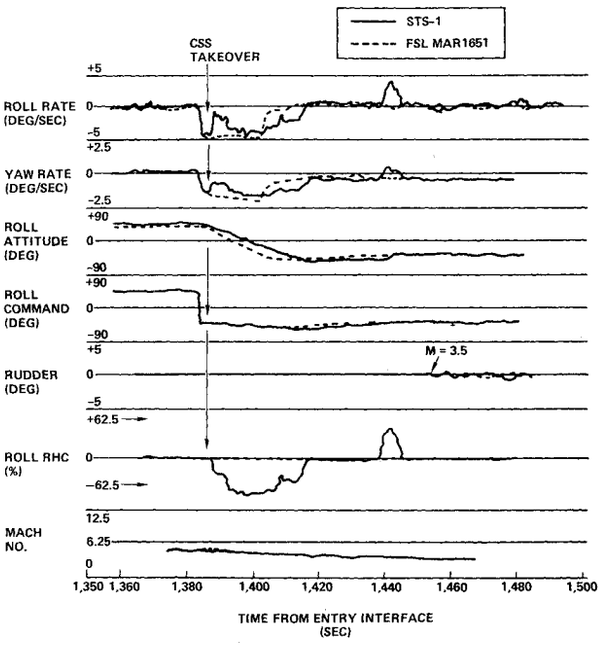

Fig. 18 Third reversal.

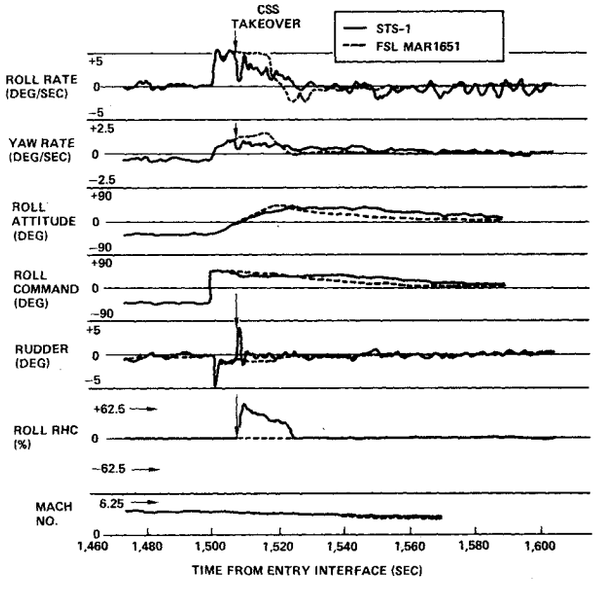

Fig. 19 Fourth reversal.

roll effectiveness in the Mach 2 to 1 region, which resulted in a low-amplitude ¼ Hz oscillation within the yaw jet deadband. This anomaly is currently under further investigation by the aerodynamic group. The static pitching moments and lift-to-drag ratio had no impact on flight control performance, but resulted in mild trajectory and surface trim deviations. The first roll maneuver low damping response, shown in Fig. 15, has been attributed to the yaw jet aerodynamic interaction, which was found to be less than the predicted lower uncertainty bound in the low ($\bar{q} \leq 15$ psf) dynamic pressure region. Stability analyses have confirmed this roll behavior in auto but not in control stick steering (CSS). Consequently, future flights have been flown in CSS through the first roll maneuver with good response. A filter on the sideslip angle feedback will be implemented on the fifth flight, which will make the auto response insensitive to yaw reaction jet aero interaction uncertainties, as shown in Fig. 16. Comparison of predicted time response from the FSL for the second, third,

and fourth roll reversals are shown in Figs. 17-19. Good comparison is evident from these figures during the initial time response of the bank reversal with auto engaged. As indicated in Fig. 17, the guidance phase change from equilibrium glide to constant drag occurred 13 sec earlier than predicted. The dynamic response to the step bank command from the second roll reversal matches well with the predicted response in FSL. At the third and fourth bank reversals, the predicted to flight dynamic response compares well until the planned manual CSS takeover occurs. This results in the transient shown in Figs. 18 and 19, as created by the initial roll rate command of zero that was set by the initial position of the rotation hand controller (RHC).

Conclusions

The first flight test of the Space Shuttle entry flight control system demonstrated nominal trajectory and nominal aerodynamics with the exception of a few off-nominal aerodynamic flight conditions which were found to be less than predicted. Good overall comparison was obtained between predicted time responses and the flight test results. Subsequent flights with flight-derived aerodynamic simulation testing have been flown with good responses. The overall flight control verification process was successful and provided assurance that the FCS would function when tested with a composite of off-nominal flight conditions.

References

[1] *Integrated Guidance, Navigation, and Control Primary Flight System Verification Plan Descent,* Rockwell International, Downey, Calif., SD 78-SH-0145B, Vols. 1, 2, and 3, Sept. 1982.

[2] *Aerodynamic Design Data Book,* Rockwell International, Downey, Calif., SD 72-SH-0060, Vol. 1, Pt. 2, April 1982.